

Metamorphic evolution of a garnetiferous mafic granulite from north-eastern segment of Chotanagpur Granite Gneissic Complex, India

*Thesis submitted for the partial fulfillment of
MSc degree in Applied Geology 2018-19*

Subho Mukhopadhyay

Roll no- MGEO194011

Department of Geological Sciences

Jadavpur University

Under the guidance of

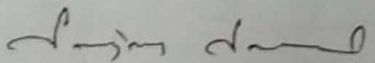
Prof. Sanjoy Sanyal



CERTIFICATE FROM THE SUPERVISOR

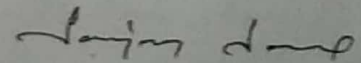
This is to certify that **Mr. Subho Mukhopadhyay** has worked under the supervision of Prof. Sanjoy Sanyal in the Department of Geological Sciences, Jadavpur University and completed his thesis entitled "**Metamorphic evolution of a garnetiferous mafic granulite from the north eastern segment of Chotanagpur Granite Gneissic Complex, India**" which is being submitted towards the partial fulfillment of his M.Sc. Final Examination in Applied Geology of Jadavpur University in 2019.

Signature of the Supervisor:


30.05.2019

Prof. Sanjoy Sanyal
Dept. of Geological Sciences
Jadavpur University
Dr. Sanjoy Sanyal
Professor
Department of Geological Sciences
Jadavpur University
Kolkata: 700032, India

Signature of Head of the Department:


30.05.2019

Prof. Sanjoy Sanyal
Dept. of Geological Sciences
Jadavpur University

Head
Department of Geological Sciences
Jadavpur University
Kolkata-700032

Contents

Abstract

Mineral abbreviations

1. Introduction.....	1
2. Background geology.....	2-4
3. Lithology.....	5-9
3.1. Felsic units	
3.2. Mafic units	
3.3. Pelitic units	
4. Petrography.....	10-12
5. Mineral chemistry.....	13-20
5.1. Analytical techniques	
5.2. Composition of different phases	
6. Mineral evolution.....	21-24
7. Geothermobarometric calculations.....	25-26
8. Discussion.....	27-34
8.1 Plotting the different metamorphic assemblages in the P-T field	
8.2. Constructing the probable P-T path	
8.3. Tectonic implication	
Acknowledgement.....	35
References.....	36-38

Abstract

The studied area Massanjore near Dumka district lies in the north-eastern part of the Chotanagpur Granite Gneissic Complex where mafic granulites occur as enclaves within the host felsic gneisses that form the major country rock. These mafic granulites develop a planar fabric mainly defined by the diagnostic mineral assemblage of high pressure granulite metamorphism (garnet + clinopyroxene + amphibole + plagioclase + quartz + rutile + ilmenite). The earliest discernable mineral assemblage includes amphibole + clinopyroxene + plagioclase + quartz + rutile occurring as inclusions in garnet porphyroblasts which form the early M_0 stage. Subsequently the assemblage garnet + clinopyroxene + plagioclase + quartz + rutile formed during the peak condition of metamorphism (M_1) defines the pervasive fabric. Conventional geothermobarometric calculations from the data of mineral chemistry yield $820 \pm 30^\circ \text{C}$ and $12 \pm 0.8 \text{ kbar}$ for the M_1 stage. The P-T estimations of the peak metamorphic assemblage suggest a steep geothermal gradient with $dP/dT \sim 71^\circ\text{C/kbar}$ that corresponds with the geothermal gradient of collisional orogeny. During the early retrograde stage (M_{IR1}) garnet breaks down to form symplectic intergrowth of clinopyroxene + plagioclase which form along the grain boundaries of garnet grains. In the late retrograde part amphibole is seen to replace the garnet and clinopyroxene grains along boundaries and fractures. These textural studies supportive with geothermobarometric calculations show a steep decompressional early retrograde path (M_{IR1} $dP/dT \sim 50^\circ\text{C/kbar}$) from the peak followed by a late retrograde event (M_{IR2} $dP/dT \sim 40^\circ\text{C/kbar}$) showing consistent cooling along with hydration. From the above information a CW P-T path is generated and the calculated peak condition 20°C/km plots in the field of high pressure granulite metamorphism. All these results are consistent with a continent-

continent collisional set up and this leads to the fact that a large part of CGGC behaved as a coherent lower plate during the globally extensive convergent margin orogenesis at the time of formation of the supercontinent Rhodinia.

Mineral abbreviations

Grt: Garnet

Cpx: Clinopyroxene

Amp: Amphibole

Pl: Plagioclase

Qz: Quartz

Ilm: Ilmenite

Rt: Rutile

1. Introduction

Appearance of the diagnostic assemblage garnet + clinopyroxene + plagioclase + rutile + quartz in mafic granulites is traditionally considered as the most reliable indicator of high pressure metamorphism (Green and Ringwood, 1967; O'Brien and Rötzler, 2003; Pattison, 2003; Zhao et al., 2001). Owing to their bulk compositions, mafic granulites develop a plethora of mineral assemblages and reaction textures in response to the changing physicochemical conditions. These can be used to constrain the P-T path that can provide clues to the tectonic processes through which the rocks have evolved.

This study mainly deals with the mafic granulites reported from the north-eastern part of the Chotanagpur Gneissic Complex and their evolution with respect to this province. A detailed background geology and lithological study (field relations) have been included here. The main objectives of my study are:

1. To identify the different mineral textures and interpret the possible reactions.
2. To prepare a detailed phase chemistry of the rock.
3. To calculate peak conditions of metamorphism as well as the P-T conditions during retrogression using conventional geothermobarometers.
4. To plot the different assemblages in the P-T space and generate a probable P-T path.
5. To explain the possible tectonic setup of the area in close relation to the rock history.

2. Background geology

The Chotanagpur Granite Gneissic Complex(CGGC) forms an important part of the East Indian Shield, along with the Archaean Singhbhum Craton, which is separated from the CGGC by the Palaeoproterozoic, North Singhbhum Fold Belt, which trends E-W to NW-SE. The CGGC is recognized as a mobile belt, belonging to the part of Central Indian Tectonic Zone(CITZ), an E-W–trending regional suture, through which major Indian blocks got stitched together in Palaeo-Neoproterozoic time (e.g. Acharyya, 2003; Bhowmik et al.,2012). However, the omnipresence of Phanerozoic sediment cover, in the western part of the CGGC ,prevents further detailed correlations between the CGGC and the Central Indian Tectonic Zone. Gangetic alluvium spreads over the northern part of CGGC, whereas the eastern margin of the terrain is covered by Phanerozoic sediments of Bengal Basin and Rajmahal Trap volcanics.

Previously published geological and geochronological data, by Sanyal and Sengupta (2012), reveals that porphyritic granitoids and charnockites (pyroxene-bearing granitoids), together termed as “felsic orthogneiss”. This comprises the major country-rock of the terrain , with several enclaves of different rock types, that vary in lithology, from mafic granulites, khondalites (i.e., garnet-sillimanite gneiss), calc-silicates , even to minor quartzite. A large body of a massif-type anorthosite, better known as the Bengal Anorthosite, is located in the southeastern part of the terrain (Chatterjee et al., 2008). Several alkaline bodies have intruded the felsic orthogneisses in the southern part of the terrain, near the North Purulia Shear Zone (NPSZ) and the South Purulia Shear Zone(SPSZ).

Indications of the presence of three major phases of deformation & metamorphism (MI, MII, MIII) ,experienced by the CGGC, can be ascertained from the geochronological and petrological data published till date (Chatterjee et al.,

2010; Ghosh and Sengupta, 1999; Maji et al., 2008; Mukherjee et al., 2017; Sanyal and Sengupta, 2012). Meta-pelitic enclaves record the oldest metamorphic event represented by an ultra-high temperature metamorphism (UHT) at moderate pressure (8 kbar) (Sanyal and Sengupta, 2012), which culminated at ~ 1650 Ma (Dey et al., 2017). The porphyritic granite intruded into the northern and western part of the terrain within 1750 Ma and 1660 Ma (Chatterjee and Ghose, 2011; Saikia et al., 2017). U-Pb zircon data estimate an age of 1550 ± 12 Ma as the emplacement age of the massif anorthosite in the south-eastern part (Chatterjee et al., 2008). Magmatism in the eastern part of the terrain extended further into the Mesoproterozoic, as revealed by the intrusion of syenite body near Dumka, that yielded a Rb-Sr age of 1475 ± 63 Ma (Ray Barman and Bishui, 1994).

The most pervasive metamorphic event, affecting the CGGC, as evident from different lithological units, occurred under high-pressure upper-amphibolite to granulite-grade conditions with peak P-T of around $750\text{--}800$ °C and $9\text{--}11$ kbar, reflecting a phase of continent–continent collision that took place around $1200\text{--}950$ Ma (Chatterjee and Ghose, 2011; Karmakar et al., 2011; Maji et al., 2008; Mukherjee et al., 2017; Rekha et al., 2011). Subsequent intrusion of mafic dykes was followed by an amphibolite grade metamorphic event ($600\text{--}750$ °C at 7 ± 1 kbar; Sanyal and Sengupta, 2012) that occurred between $870\text{--}780$ Ma (Chatterjee et al., 2010; Sanyal and Sengupta, 2012). However, Chatterjee et al. (2010) inferred this event as a high-grade metamorphism reaching a pressure of ~ 12 kbar at 730 °C associated with the Eastern Indian Tectonic Zone (EITZ). Detailed geochemical data of the granitoids are scarce from the vast terrain and only reported by few workers (Goswami and Bhattacharyya, 2013; Lalnunmawia et al., 2011; Saikia et al., 2017; Singh and Krishna, 2009; Yadav et al., 2014).

Porphyritic granites near Gaya are characterized as A-type granites formed by the high-temperature melting of lower to middle crust with varying mantle input

(Yadav et al., 2014) and has intruded at 1697 Ma (Chatterjee and Ghose, 2011). On the contrary, granites in the north-western part are inferred to be arc-related magma, which intruded between 1750–1660 Ma (Saikia et al., 2017).

My study area is Massanjore, which is located in the eastern part of CGGC, at the southern tip of Dumka District, in Jharkhand.

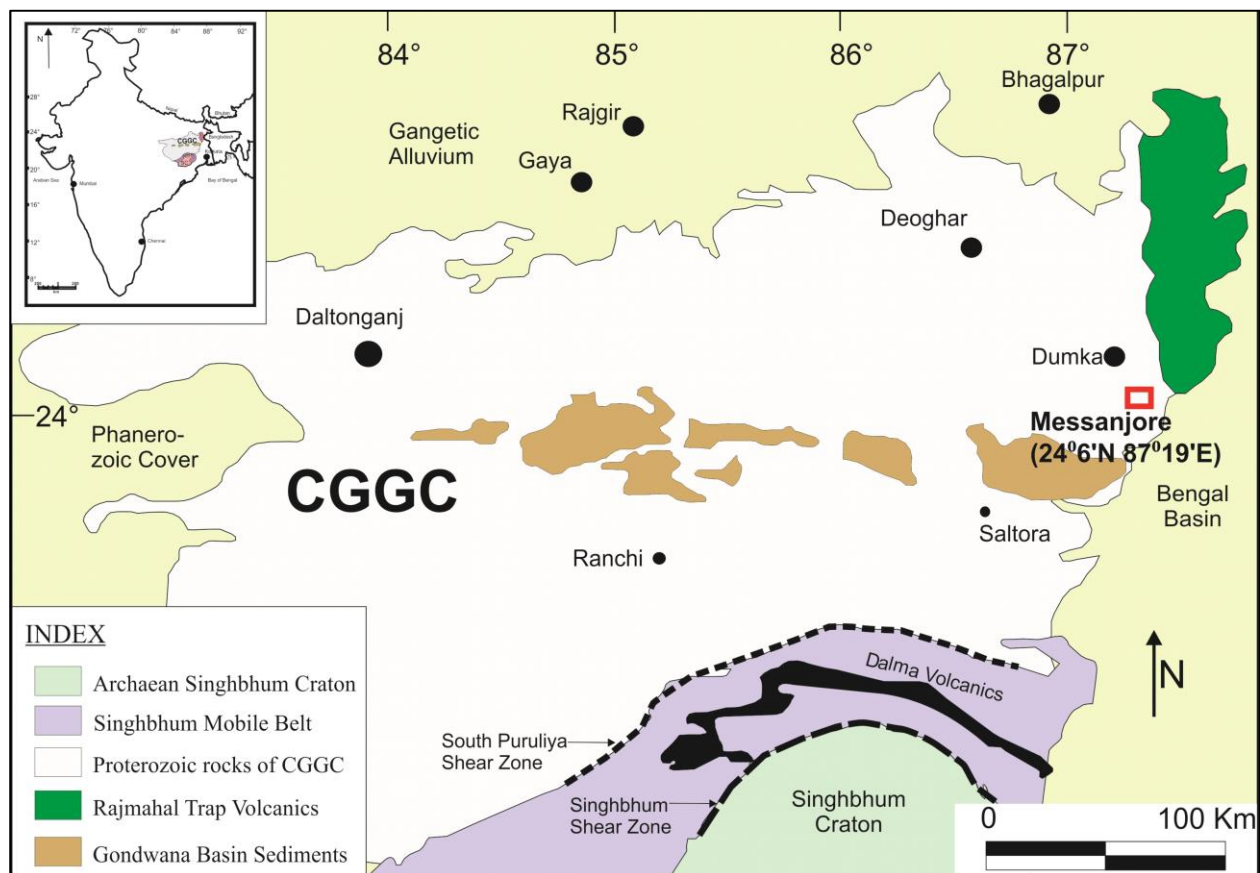


Fig (1) Geological map of the CGGC and part of the Singhbhum mobile belt (SMB) modified after Acharya, 2003. Square box shows the studied area located in the north-eastern part of the

3. Lithology

Masanjore is situated at the eastern margin of CGGC in the district of Dumka, Jharkhand. The rock units in these areas are spatially distributed covering Ranishawr-Sadipur Murjora-Ranibahal area, Dam area, Bagnal and extending upto Patabari and Ragnali-Asanbani area. The major rock type in and around Massanjore, Jharkhand broadly is felsic in nature. It mainly consists of three types of felsic units. These felsic units include an augen gneiss or porphyritic granite, a migmatitic gneiss and a leucogranite. Apart from these felsic units which form the country rock of the area other metapelitic bodies and mafic units are present within the country rock as enclaves or intrusive bodies. Studying the different rock types and the structures shown by them help to understand the deformation history of the area and its relationship with the evolution of the Chotanagpur Gneissic Complex.

3.1. Felsic units:

Coming to the descriptive part of the different felsic units observed and studied in and around Massanjore area we have to deal with three rock units. The most abundant and major rock unit forming the country rock of the area is the migmatitic felsic gneiss. Though overall the rock is medium to fine grained, it is highly banded and these leucosomal bands consisting of quartz and feldspars are comparatively coarser than the host rock unit. Beads of garnets are present within this leucosomal banding along with its host. But again, garnets are coarser and more abundant in the leucosomal part. This rock is a partially melted migmatitic gneiss and shows upto third generation of folding. The trend and plunge of fold axis F_2 : $37^\circ \rightarrow 110^\circ$. The

rock unit shows thickened hinge areas and pinch and swell structures in the limb part. White rims around garnet grains can be seen Pic. Clinopyroxene is present in the rock unit. Sometimes this rock type showed thinly banded nature and an overall charno-enderbitic composition. The general trend of F_3 fold axis is 155° . Laterally continuous bands associated with S_2 are seen and this entire unit is intruded by a mafic dyke. F_1 and F_2 folds are coaxial.

The rock shows a spotted nature, consisting of large potash feldspar grains, jacketed with quartz and garnet. The rock shows a bluish gray colour, and a greasy appearance, typical of a charno-enderbitic rock. The feldspar grains are quite large in size and show typical butterfly twinning indicating its igneous origin. Garnet appears as a chain like structure around the stretched feldspar porphyroclasts. Amphibole grains also form a jacket around the feldspar grains and are distributed throughout the rock. Enclaves of the felsic country rock present within this rock body implies its later intrusion compared to the other. In some places, the rock seemed to have some folded pegmatitic veins and at some other places amphibolite enclaves. The bluish grey colour is mainly due to the presence of blue quartz in the rock. The rock shows clear evidences of deformation. The large feldspar grains are stretched along with their halo and gives an eye shaped appearance, which compels us to acknowledge them as feldspar augens. The stretching of feldspar grains only indicate a high temp metamorphic event. So, the once emplaced porphyritic granite was metamorphosed to form Augen Gneiss. In several exposures, the augen gneiss shows to have enclaves of mafic rock and the migmatitic felsic gneiss. The S_1 plane of the feldspar augen gneiss coincides with the S_2 .

The last major felsic rock type is a leucogranite. This rock is highly deformed and contains elongated grains of biotite on the foliation plane giving it a streaky appearance also called as streaky gneiss with two prominent layers of fine and coarse

grains. The leucosomes contain some mafic minerals. All these three rock units are later intruded by a coarse-grained pegmatitic unit.

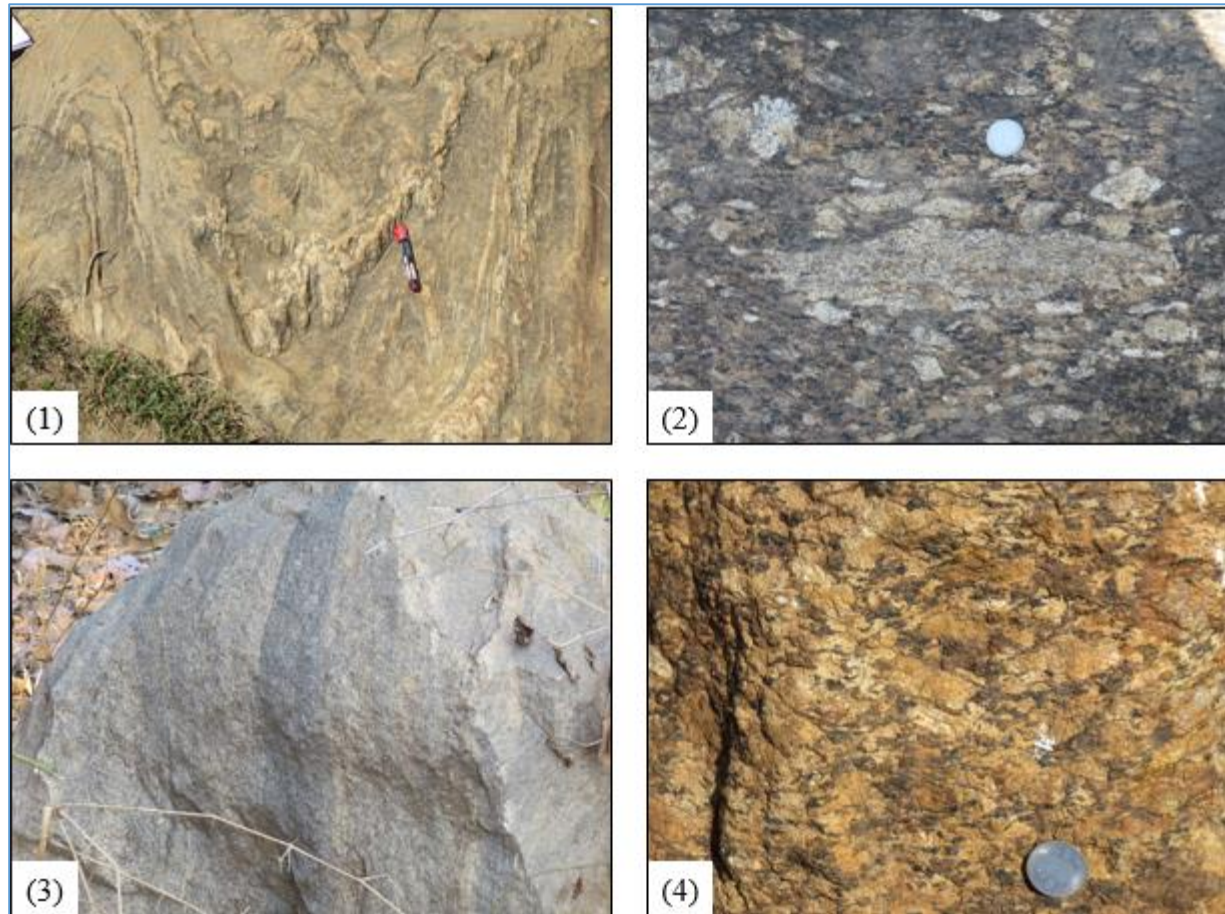


Fig (2) 1. Host migmatitic gneiss 2. Elongated feldspar grains of Augen gneiss 3. Leucogranite or streaky gneiss 4. Amphibole along feldspar grains of Augen gneiss

3.2. Mafic units:

The mafic granulite body is present as an enclave within this felsic country rocks. Amphibole, pyroxene, garnet and plagioclase are the major constituent minerals of this mafic rock. Due to the variation in grain size this rock can be divided into two types. The first type encountered is a host mafic granulite medium to fine-grained with various other features. The rock is well-foliated with a general trend of 220°

and containing good amount of garnet grains. The foliation is defined by the amphibole grains. These garnet grains occur as clusters are small in size. The rock is very hard in nature patches of melts are also present within the host rock type. The next type is a similar to the first type with very large pinkish red garnet grains spread throughout the rock unit, also called as measles garnet. Around the garnet grain a halo of amphibole and plagioclase is formed. Feldspathic veins are present within the rock body. Some feldspathic veins are coarse grained and contains amphibole and profuse garnets. These veins are quite thick (5 to 6 cm). Apart from this some thin feldspathic veins are present which are garnetiferous.

Another mafic rock type is that of an amphibolite with felsic veins in some areas. The rock is medium to fine-grained. In some places this deformed basic rock contains veins of pyroxene. The pyroxene veins are sometimes folded and the foliations of the host basic rock cut the hinge parts of these small scale folds. The general foliation trend is 185° .

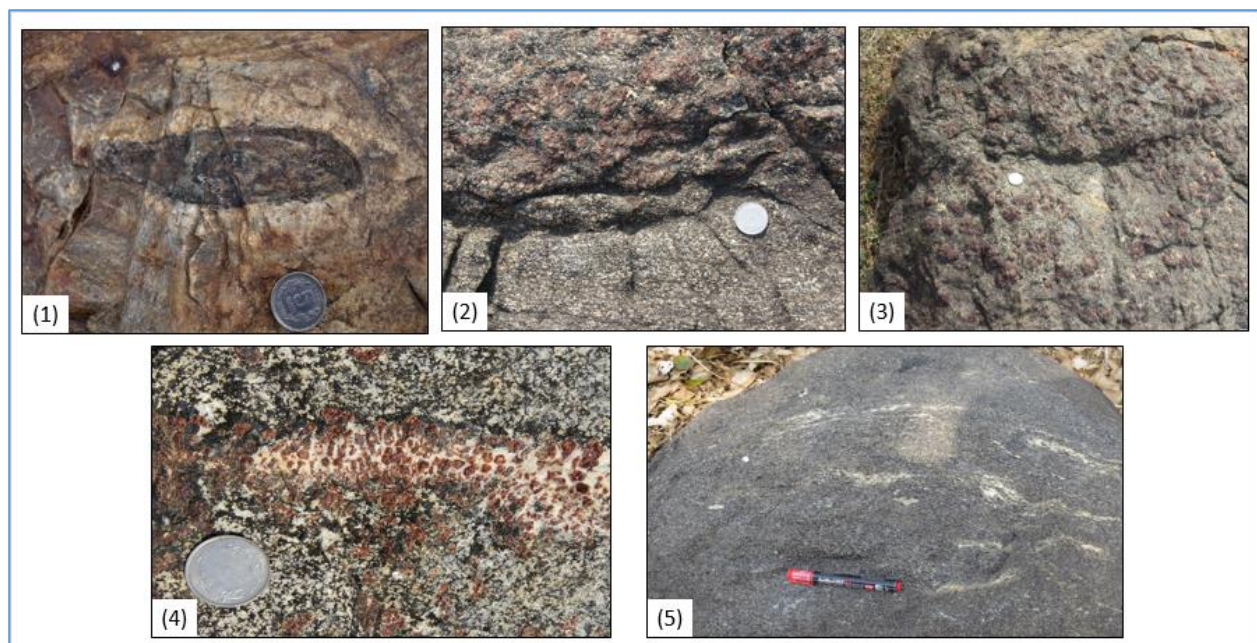


Fig (3) 1. Mafic enclave in host felsic gneiss 2. Clusters of small garnet grains in mafic granulite 3. Measles-like garnet in mafic granulite 4. Wall-controlled growth of garnet in a vein intruding the host mafic unit 5. Amphibolite with felsic veins

3.3. Pelitic units:

Two major pelitic rock bodies are also present. One of them shows evidence of profuse melting and forms leucosomal bands which contain large clusters of garnets. These leucosomal bands are medium to coarse grained parts of quartz and K-feldspar. Needle like sillimanite grains are also present.

The other pelitic body lacks this kind of leucosomal bands and overall more fine grained and more homogenous than the former one. Along with garnet, cordierite is also present within this rock and gives it a deep blue tinge.

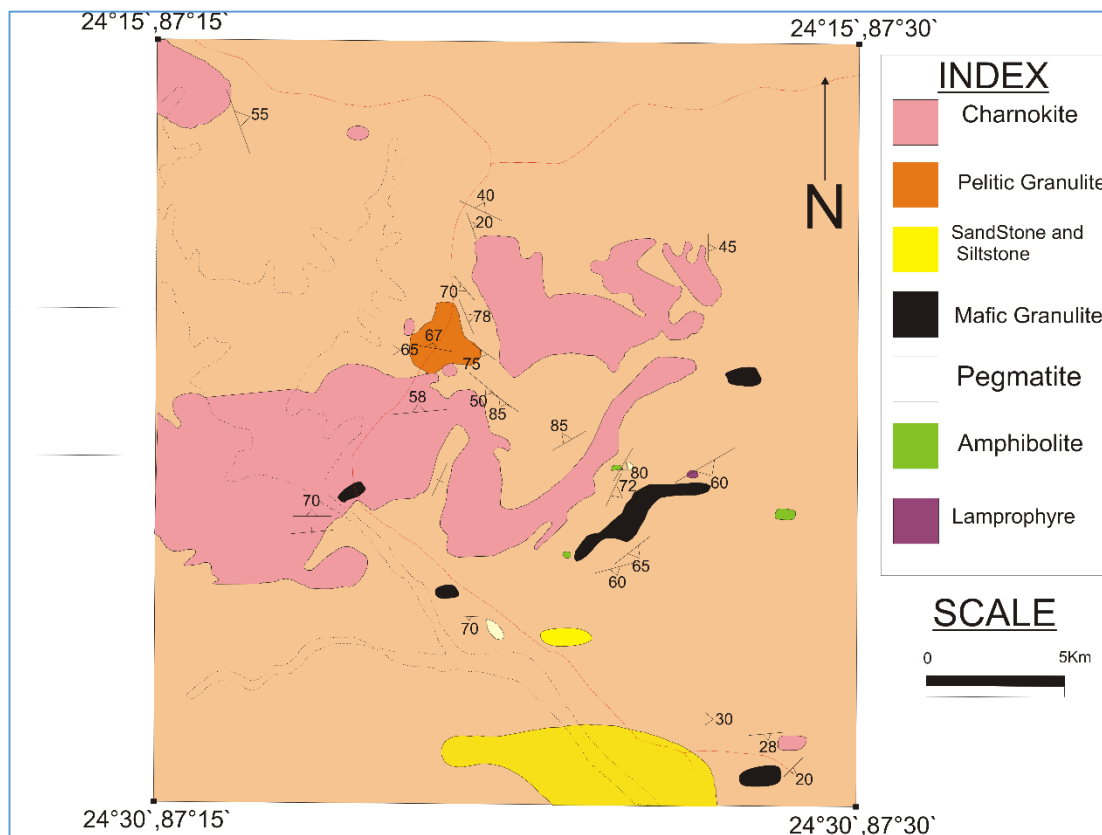


Fig (4) Lithological map of the studied area

4. Petrography

Overall Description:

The studied thin sections reveal that the rock is mafic in nature and it is overall coarse to medium grained. The dominant minerals are garnet, clinopyroxene, amphibole, plagioclase, quartz and also ilmenite, rutile and sphene are present in little amounts scattered throughout different parts of the slide. The grains are oriented and in many places show recrystallized boundaries.

The **peak assemblage (pic)** of the rock consists of large porphyroblastic garnet grains, subhedral clinopyroxene grains, plagioclase laths and recrystallized quartz grains.

The garnet porphyroblasts consist of different kinds of inclusions of other minerals like quartz, plagioclase and sometimes amphibole also. The garnet grains are heavily fractured and along the boundaries of the garnet grains symplectitic intergrowth of clinopyroxene and plagioclase grains are present. Another striking feature is the garnet breakdown reaction forming double corona with clinopyroxene and plagioclase.

Petrographically clinopyroxene is present in two modes. Clinopyroxene grains (Cpx1) are present as large subhedral grains in the peak assemblage along with garnet porphyroblasts. In the second mode clinopyroxene grains are present as symplectites with plagioclase along the grain boundaries of garnet and in some cases this garnet breakdown reaction forms double corona of plagioclase and clinopyroxene separating garnet grains from the adjoining quartz. The clinopyroxene grains show two sets of cleavage, higher order blue-green interference colours and very weak pleochroism in plane polarized light.

Similarly plagioclase also forms in two modes. Matrix and coarse plagioclase (Pl1) associated with the peak assemblage of garnet and clinopyroxene (Cpx1). The other mode (Pl2) is associated with the garnet breakdown assemblage. Apart from these as mentioned above inclusions of plagioclase is also found in garnet porphyroblastic grains. The other mineral that is present as inclusion within the garnet profusely is quartz. It is also present in the matrix taking part in the garnet breakdown reaction.

Amphibole grains are present as large anhedral to subhedral highly pleochroic grains. Inclusions of amphibole are present within the garnet porphyroblasts. But most are prominently replacing all of the ferromagnesian phases. The amphibole grains are mainly replacing the clinopyroxene grains. Amphibole grains replace both Cpx1 and Cpx2. They replace the clinopyroxene grains either from the boundary or along the cleavage plane. Relicts of the clinopyroxene grains are present along the cleavage planes due to partial replacements. They also replace the garnet grains along the grain boundaries and also along the fracture planes.

Some opaque phases like ilmenite and rutile are also present in minor amounts sometimes as inclusions in garnet grains also show less modal abundance in peak assemblage. Other accessory phases i.e. apatite, sphene are also present in the matrix.

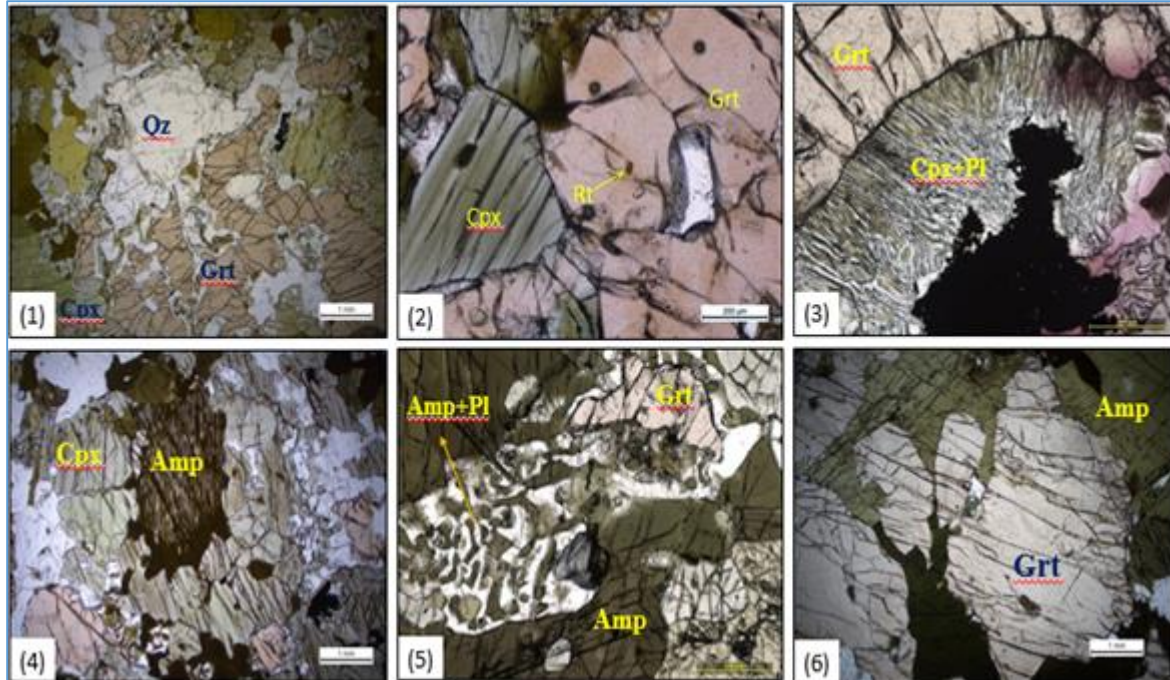


Fig (5) 1. Overall rock 2. Inclusions in garnet 3. Garnet breaks down to form Cpx-Pl symplectic intergrowth 4. Amphibole replacing clinopyroxene 5. Garnet breaks down to form Amp-Pl symplectic intergrowth 6. Amphibole replacing garnet along boundaries and fractures

5. Mineral chemistry

5.1. Analytical techniques:

Major elemental analyses were performed using a Cameca SX100 Electron Probe Micro Analyser equipped with four wavelength-dispersive spectrometers (WDS) from the Department of Geology and Geophysics, Indian Institute of Technology, Kharagpur. All points were analysed with 15 kV acceleration voltage, 20 nA beam current and a beam size of 1 mm. The dwell time for the measured elements was set at 10 s for the peak and 5 s for the background. Natural minerals and synthetic compounds were used as standards.

Compositions of the minerals from mafic granulite sample were analysed and the mole fractions of different components were calculated from the data. During cation recalculation from oxide weight percentage, Fe⁺³ was calculated after the scheme of Droop (1987).

Representative mineral compositions are presented in tables. Mineral abbreviations in figures and tables have been used after Whitney and Evans (2010). In the following section, salient compositional features of the minerals are described.

3.2. Composition of different phases:

Garnet

Garnet in the studied rock is a solid solution of pyrope-almandine-grossular, with minor spessartine. There is a variation in composition of garnet grains from core to rim. The rims are comparatively Fe-rich than the core part of the garnet with Alm values ranging from 0.56 to 0.49. The core parts are more Mg-rich (pyrope) with values varying from 0.238 to 0.2. The rim parts show lower grossular content than core where values reach almost up to 0.2855 with a few exceptions where the value is higher in the rim parts. A decrease in Mg + Ca towards the rim appears to be compensated by an increase in $\text{Fe}^{+2} + \text{Mn}$.

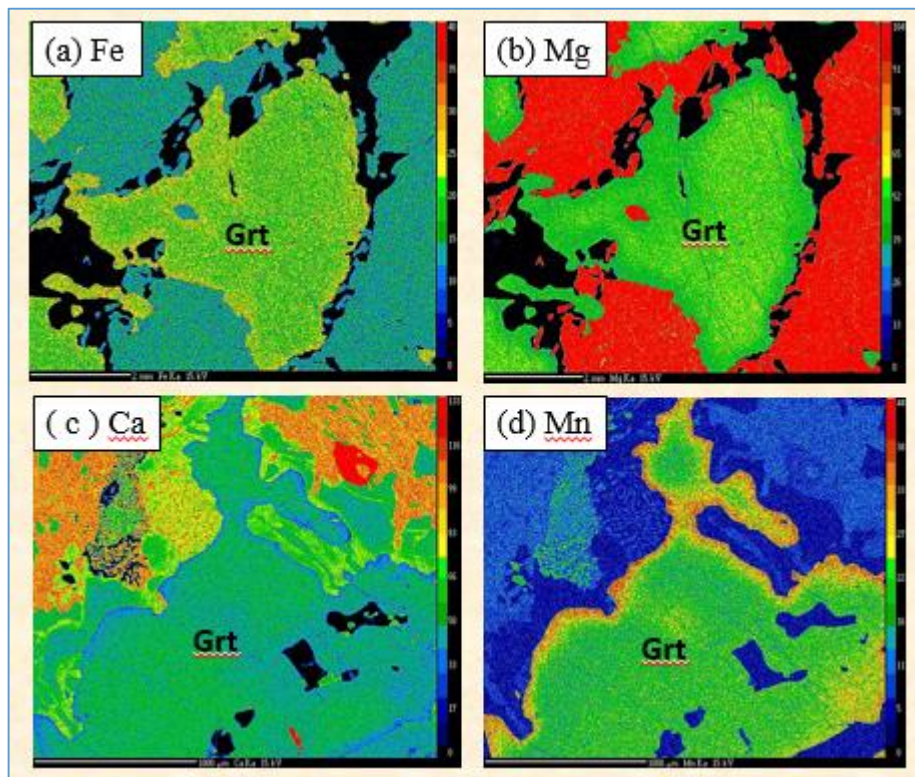


Fig (6) X-ray intensity elemental maps.

Clinopyroxene

Representative clinopyroxene data of the porphyroblastic (Cpx1) and symplectic pyroxenes (Cpx2) are presented in Table . Both of the porphyroblastic and symplectic clinopyroxene grains are typically diopsidic in nature. $X_{Mg}=0.731-0.8151$. The clinopyroxene grains forming the different symplectites do not show much variation in X_{Mg} values (0.768-0.81) and Al_2O_3 content shows a reasonable amount of variation. Cpx1 has an alumina content of about 4-6 wt%. Compared to Cpx1, symplectic clinopyroxenes are less aluminous (value) and the FeO contents range from 8.6 to almost 12 wt% with no proper variation trend between the two types of clinopyroxene. TiO_2 content is very low not exceeding 0.628 wt%. No proper decreasing or increasing trends of X_{Mg} from core to rim are noticed in the porphyroblastic Cpx1.

Plagioclase

Representative plagioclase compositions are given in Table 3. There is a considerable variation in plagioclase compositions depending on the textural types. Core-rim compositions of the matrix plagioclase and composition of the symplectic plagioclase forming symplectites with clinopyroxene and amphibole are represented. K-feldspar component in all the plagioclase types is less than 1%. The matrix plagioclase has an anorthite component of 43-55%. It is andesine (An 43-49%) in the core and labradorite (An 50-55%) towards the rim. But the symplectic plagioclase is considerably more anorthitic bytownite (An 73-83%). The plagioclase grains included within garnet porphyroblasts have higher anorthitic values (An₆₁Ab₃₈).

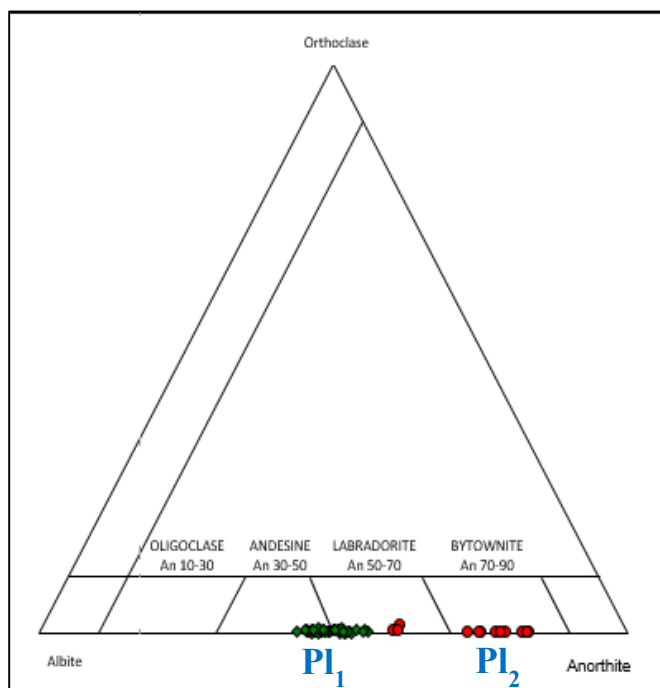


Fig (7) An-Alb component plot showing variation in composition of Pl₁ and Pl₂.

Amphibole

Representative chemical compositions of the matrix amphiboles, symplectic amphiboles (Pl+ Amp \pm Ilm symplectites), and amphibole inclusions in garnets are presented in Table 4. According to the classification scheme of Leake et al (1997-2004) compositions of all the amphiboles are calcic in nature with X_{Mg} values ranging from 0.63-0.72. The amphibole grains included in garnet have X_{Mg} value of 0.66. The TiO_2 in amphibole ranges from 0.024-2.028 wt %. There is no prominent variation in composition from core to rim in the prismatic matrix amphiboles.

Other/accessory minerals

Ilmenite, rutile and quartz have near-stoichiometric compositions.

Table (1). Representative chemical analyses of Amphibole

	Am	Am replace cpx	Am sym	Ap in cpx1
DataSet/Point	61 / 1	63 / 1	5 / 1	7 / 1
Na2O	1.621	1.702	1.569	0.036
F	0	0	0	2.047
MgO	13.903	12.955	12.993	0
Cl	0.005	0.022	0.015	0.265
P2O5	0.107	0.015	0.031	42.205
K2O	0.277	0.303	0.313	0
CaO	11.721	11.893	11.805	56.001
TiO2	1.608	1.678	1.562	0.027
Cr2O3	0	0.08	0.028	0.005
MnO	0	0.107	0.149	0
FeO	13.596	14.936	13.715	0.059
ZnO	0	0.408	0.157	0
BaO	0.013	0.004	0	0
Al2O3	10.018	10.418	10.547	0
SiO2	45.693	45.153	45.996	0.026
Total	98.562	99.674	98.88	100.672
XMg	0.72	0.68	0.67	0
XFe	0.28	0.32	0.33	0

Table (2). Representative chemical analyses of Plagioclase

	Pl1 core	Pl1 core big	Pl core	Pl rim	Pl1 rim	Pl2 sym
DataSet/Point	64 / 1 .	11 / 1 .	56 / 1 .	57 / 1 .	60 / 1 .	4 / 1 .
Na2O	6.009	2.595	6.765	5.635	6	2.406
F	0	0.033	0.015	0.027	0	0
MgO	0.002	0.004	0	0.011	0.003	0
Cl	0.009	0.004	0.003	0	0.01	0
P2O5	0	0.024	0.033	0.001	0.01	0.03
K2O	0.079	0.01	0.097	0.043	0.09	0.021
CaO	10.565	16.464	9.481	10.98	10.422	16.754
TiO2	0.005	0.067	0.011	0	0	0
Cr2O3	0	0	0.1	0.004	0.009	0.015
MnO	0	0	0.02	0.125	0.008	0.01
FeO	0.065	0.127	0.067	0.108	0.022	0.039
ZnO	0	0	0	0.039	0	0
BaO	0.01	0	0	0	0.009	0.009
Al2O3	28.3	32.961	26.983	28.154	27.78	33.252

SiO ₂	55.792	48.655	57.066	54.907	55.385	48.373
Total	100.836	100.942	100.641	100.033	99.749	100.909

	Pl1 core	Pl1 core big	Pl core	Pl rim	Pl1 rim	Pl2 sym
DataSet/Point	64 / 1 .	11 / 1 .	56 / 1 .	57 / 1 .	60 / 1 .	4 / 1 .
Na	0.521	0.229	0.587	0.494	0.526	0.212
F	0.000	0.005	0.002	0.004	0.000	0.000
Mg	0.000	0.000	0.000	0.001	0.000	0.000
Cl	0.001	0.000	0.000	0.000	0.001	0.000
P	0.000	0.001	0.001	0.000	0.000	0.001
K	0.005	0.001	0.006	0.002	0.005	0.001
Ca	0.506	0.802	0.454	0.531	0.505	0.816
Ti	0.000	0.002	0.000	0.000	0.000	0.000
Cr	0.000	0.000	0.004	0.000	0.000	0.001
Mn	0.000	0.000	0.001	0.005	0.000	0.000
Fe	0.002	0.005	0.003	0.004	0.001	0.001
Zn	0.000	0.000	0.000	0.001	0.000	0.000
Ba	0.000	0.000	0.000	0.000	0.000	0.000
Al	1.492	1.766	1.422	1.499	1.480	1.782
Si	2.495	2.212	2.552	2.480	2.503	2.199
Anorthite	49.030	77.710	43.36	51.7	48.750	79.300
Albite	50.480	22.190	56.060	48.100	51.270	20.600
Orthoclase	0.484	0.097	0.573	0.195	0.483	0.097
Total	99.994	99.997	99.993	99.995	100.503	99.997

Table (3). Representative chemical analyses of Garnet

	Grt core	Grt int	grt core	Grt rim	Grt rim	Grt rim
DataSet/Point	1 / 1 .	2 / 1 .	25 / 1 .	3 / 1 .	17 / 1 .	32 / 1 .
Na ₂ O	0.005	0.000	0.017	0.030	0.000	0.045
F	0.000	0.000	0.000	0.000	0.000	0.000
MgO	5.781	5.823	6.128	4.157	4.933	4.831
Cl	0.016	0.014	0.000	0.004	0.023	0.000
P ₂ O ₅	0.053	0.083	0.000	0.038	0.042	0.040
K ₂ O	0.000	0.000	0.000	0.001	0.000	0.000
CaO	11.696	11.863	11.321	11.414	9.304	8.997
TiO ₂	0.151	0.144	0.104	0.184	0.066	0.010
Cr ₂ O ₃	0.000	0.000	0.000	0.014	0.081	0.054
MnO	0.799	0.716	0.749	1.184	1.124	1.646

Fe2O3	1.069	1.571	2.847	2.301	2.984	2.708
FeO	21.268	20.773	20.516	22.607	24.060	23.803
ZnO	0.152	0.000	0.000	0.000	0.000	0.000
BaO	0.000	0.000	0.000	0.000	0.028	0.000
Al2O3	21.893	21.601	21.897	21.247	21.341	21.627
SiO2	39.621	39.191	39.043	38.271	38.402	38.240
Total	102.504	101.779	102.622	101.453	102.388	102.001

	Grt core	Grt int	grt core	Grt rim	Grt rim	Grt rim
DataSet/Point	1 / 1 .	2 / 1 .	25 / 1 .	3 / 1 .	17 / 1 .	32 / 1 .
Na	0.001	0.000	0.002	0.004	0.000	0.007
F	0.000	0.000	0.000	0.000	0.000	0.000
Mg	0.649	0.659	0.688	0.478	0.563	0.553
Cl	0.002	0.002	0.000	0.001	0.003	0.000
P	0.003	0.005	0.000	0.002	0.003	0.003
K	0.000	0.000	0.000	0.000	0.000	0.000
Ca	0.944	0.965	0.914	0.944	0.764	0.741
Ti	0.009	0.008	0.006	0.011	0.004	0.001
Cr	0.000	0.000	0.000	0.001	0.005	0.003
Mn	0.051	0.965	0.048	0.077	0.073	0.107
FeIII	0.061	0.090	0.161	0.134	0.172	0.157
Fe	1.341	1.319	1.293	1.460	1.542	1.530
Zn	0.008	0.000	0.000	0.000	0.000	0.000
Ba	0.000	0.000	0.000	0.000	0.001	0.000
Al	1.945	1.932	1.945	1.933	1.927	1.959
Si	2.986	2.975	2.942	2.955	2.943	2.939
Garnet Composition						
Prp	0.217	0.220	0.234	0.162	0.191	0.189
Grs	0.286	0.277	0.229	0.251	0.172	0.172
Adr	0.031	0.045	0.081	0.067	0.086	0.079
Alm	0.449	0.441	0.439	0.493	0.524	0.522
Sps	0.017	0.015	0.016	0.026	0.025	0.037
Total	0.999	0.998	0.999	0.999	0.998	0.999

Table (4). Representative chemical analyses of clinopyroxene

	Cpx1	Cpx	Cpx	Cpx sym	Cpx2 sym	Cpx1 rim big
DataSet/Point	62 / 1 .	67 / 1 .	69 / 1 .	59 / 1 .	9 / 1 .	13 / 1 .
Na2O	0.722	0.459	0.28	0.335	0.239	0.425
F	0.01	0	0	0	0.049	0.044
MgO	13.491	12.65	14.276	14.451	14.297	12.875

Cl	0.007	0.006	0.009	0	0.005	0.004
P2O5	0.071	0.105	0.04	0.096	0.084	0.06
K2O	0.057	0	0.028	0.014	0	0
CaO	20.2	22.739	23.266	23.657	23.367	23.257
TiO2	0.563	0.305	0.167	0.203	0.271	0.334
Cr2O3	0.063	0.031	0.157	0.006	0.029	0
MnO	0.067	0.102	0.234	0.202	0.242	0.212
FeO	10.848	11.1	9.052	8.653	9.166	9.862
ZnO	0	0	0	0.027	0	0
BaO	0	0	0.006	0	0.019	0
Al2O3	4.413	2.824	1.433	1.3	1.069	3.232
SiO2	50.318	51.289	52.364	52.98	52.79	52.118
Total	100.83	101.611	101.312	101.925	101.626	102.423

	Cpx1	Cpx	Cpx	Cpx sym	Cpx2 sym	Cpx1 rim big
DataSet/Point	62 / 1 .	67 / 1 .	69 / 1 .	59 / 1 .	9 / 1 .	13 / 1 .
Na	0.052	0.033	0.020	0.024	0.017	0.030
F	0.001	0.000	0.000	0.000	0.006	0.005
Mg	0.742	0.695	0.782	0.785	0.781	0.700
Cl	0.000	0.000	0.001	0.000	0.000	0.000
P	0.002	0.003	0.001	0.003	0.003	0.002
K	0.003	0.000	0.001	0.001	0.000	0.000
Ca	0.798	0.899	0.916	0.924	0.917	0.908
Ti	0.016	0.008	0.005	0.006	0.007	0.009
Cr	0.002	0.001	0.005	0.000	0.001	0.000
Mn	0.002	0.003	0.007	0.006	0.008	0.007
FeIII	0.114	0.100	0.096	0.086	0.092	0.078
Fe	0.220	0.243	0.182	0.178	0.189	0.222
Zn	0.000	0.000	0.000	0.001	0.000	0.000
Ba	0.000	0.000	0.000	0.000	0.000	0.000
Al	0.192	0.123	0.062	0.056	0.046	0.139
Si	1.856	1.892	1.923	1.931	1.934	1.900
XMg	0.771	0.741	0.811	0.815	0.805	0.759

6. Mineral evolution

In this section, the petrographic observations and the compositional variation of different minerals are combined to identify the different sets of mineral assemblages that developed in sample SM128A. Integrating the textural relations an attempt has been made to reconstruct the mineral reactions that occurred in the rocks as a result of the changing physicochemical conditions of metamorphism. Four sets of metamorphic assemblages have been identified on the basis of preserved textures and are taken as indicative of four stages (M_0 to M_{1R2}) of mineral evolution.

Depending on the preserved mineral assemblages and reaction texture along with the composition of various phases, mineralogical evolution of the rock is divided into four stages, i) Early assemblage (M_0), ii) Peak assemblage (M_1), iii) Early retrograde assemblage (M_{1R1}), iv) Late retrograde assemblage (M_{1R2}). Mineral assemblages of these four stages are described here.

Early Assemblage (M_0 stage)

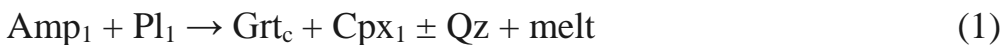
Preservation of the prograde assemblage is very poor. It is preserved only as inclusions within the garnet porphyroblasts. Plagioclase + amphibole + ilmenite \pm rutile + quartz that occur as inclusions within garnet constitute the earliest discernible assemblage. This early assemblage that constituted the rock before formation of garnet was either inherited from an older metamorphic/magmatic assemblage or formed during prograde metamorphism.

Peak Assemblage (M₁ stage)

The granuloblastic assemblage Grt_C + Cpx₁ + Pl₁ + quartz was stabilized during peak metamorphism. The reaction(s) responsible for the formation of porphyroblastic garnet cannot be uniquely deciphered due to the lack of preserved reaction textures, but can be estimated from the inclusion phases present within these garnets. Inclusions of amphibole, clinopyroxene, plagioclase, ilmenite and quartz within garnet suggest that garnet was formed through a combination of the following reactions:



The peak (M₁) condition is constituted by the assemblage of garnet (Grt_c), medium to coarse grained matrix clinopyroxenes (Cpx₁), matrix plagioclase (Pl₁), quartz and rutile. Preservation of the reaction textures that are responsible for the formation of the peak assemblage is very poor as in prograde paths, reactions tend to go to completion (ref). But the inclusions of amphibole, clinopyroxene, quartz, plagioclase within the garnet inclusions give us a glimpse at the reactions that might have occurred during the formation of the peak assemblage. The textural evidences suggest the following reactions,

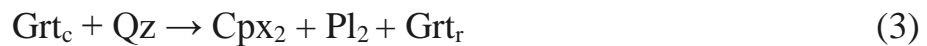


The peak metamorphic assemblage of garnet, clinopyroxene, plagioclase and quartz in metabasic rocks represents a high pressure condition in mafic granulites (Pattison, 2003; O'Brien and Rötzler, 2003; Green and Ringwood, 1967; Zhao et

al., 2001). Experimental work on MOR basalts suggest that reaction 1 is pressure sensitive, sub-horizontal with a slightly negative slope and represent a P-T condition of 9-14 kbar and 800-1000 °C (Veilzeuf & Schmidt, 2001; Liu et al., 1996; Bhowmick & Roy, 2003; and references cited there). For the reaction to move towards the right, increase of pressure is necessary with or without increase in temperature. Reaction 2 is also strongly pressure dependent and used as barometers (Newton & Perkins, 1982; Eckert et al., 1991). For the reaction to move forward increase in pressure is required (Zhao et al., 2001; Dey et al. 2018). Now both peak assemblage forming reactions are pressure sensitive and move in the forward direction with increase of pressure with a negative volume change. Judging from the size of the garnet grains (>1000 µm) the increase in pressure may was accompanied by an increase of temperature simultaneously (Carlson, 1989).

Early Retrograde Symplectic Assemblage (M_{IR1} stage)

The early retrograde assemblage is defined by the breakdown of the peak garnet (Grt_c). In few instance, Grt_c broke down to form a symplectic intergrowth of clinopyroxene (Cpx_2) and plagioclase (Pl_2). In other cases, Grt_c is rimmed by a double corona of Cpx_2 and Pl_2 separated from the quartz grains. As a result of this the rim composition of the garnets have undergone diffusional re-equilibration to form Grt_r . Textural features suggest,

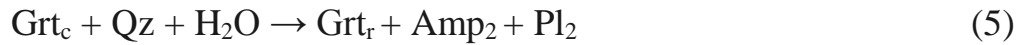


This reaction is essentially reverse with respect to the peak forming reaction (2) and will move to the right with decompression (Newton & Perkins, 1982; Essene, 1989; Zhao et al., 2001). The symplectic plagioclase (Pl_2) is much more calcic ($An=75-85\%$) than the matrix plagioclase ($An= 45-55\%$). This enrichment of the

anorthite component in Pl₂ can be counted on by the breakdown of garnets which do not have any sodic components in its structure (Dey et al., 2018; Bhowmik and Roy, 2003; Karmakar and Schenk, 2015; Liu et al., 2013, 2015; Pitra et al., 2010; Zhao et al., 2001, 1999, 2000).

Late Retrograde Hydrous Assemblage (M_{IR2} stage)

This metamorphic stage introduces hydrous phase (amphibole) in the assemblage. Amphibole (Amp₂) is replacing the anhydrous ferro-magnesian minerals (garnet, clinopyroxene) along fractures and along grain boundaries, forming a symplectic intergrowth of Amp₂ + Pl₂. Textural diagrams represent the following reactions,



Stages	Minerals present	Possible reactions
M1	Grt _c + Cpx ₁ + Pl ₁	$\text{Amp}_1 \pm \text{Qz} \pm \text{Ilm} \rightarrow \text{Grt}_c + \text{Cpx}_1 + \text{Pl}_1 \pm \text{Rt} + \text{H}_2\text{O}$ $\text{Cpx}_1 + \text{Pl}_1 \pm \text{Ilm} \rightarrow \text{Grt}_c + \text{Qz} \pm \text{Rt}$
M _{IR1}	Grt _r + Cpx ₂ + Pl ₂	$\text{Grt}_c + \text{Qz} \rightarrow \text{Cpx}_2 + \text{Pl}_2 + \text{Grt}_r$
M _{IR2}	Amp ₂ + Pl ₂ + Grt _r	$\text{Grt}_c + \text{Qz} + \text{H}_2\text{O} \rightarrow \text{Grt}_r + \text{Amp}_2 + \text{Pl}_2$ $\text{Grt}_r + \text{Qz} \pm \text{Cpx}_2 + \text{H}_2\text{O} \rightarrow \text{Amp}_2 + \text{Pl}_2$

Table (5) Different stages of evolution of evolution of the minerals

7. Geothermobarometric calculations

Petrographic study of the mafic granulites helped us to identify three distinct sets of assemblages namely a peak assemblage, an early retrograde assemblage and a late hydrous assemblage. The textures of the different stages were helpful in calculating P-T conditions using different thermometers and barometers. In the table shown below is a representation of the P-T conditions of the three different assemblages.

Stages	Assemblage	Minerals	Thermometry Method	Calculated T(°C)	P ref (kbar)	Barometry Method	T ref (°C)	Calculated P (kbar)
M ₁	Peak	Cpx1+Pl1+Gt1	GC	820±30	12	GCPS	850	12±0.8
M _{1R1}	Early retrograde <u>symplectite</u>	Cpx2+Pl2+Gt2	GC	650±25	8	GCPS	650	7.8±0.5
M _{1R2}	Late retrograde hydrous	Gt2+Amp	<u>Gt-Hbl</u>	570±40		Al in <u>Hbl</u>	570	6±0.4

Table (6) Conventional geothermobarometry

From the calculated temperatures and pressures shown in the above table it is evident that a retrogression has taken place from the peak metamorphic assemblage (M₁).

The peak metamorphic condition estimated through mineral thermobarometry analysis corresponds to the maximum achieved pressure temperature and denotes high-pressure granulite facies conditions.

Conventional thermobarometry of the peak assemblage is carried out using the core compositions of the porphyroblastic garnets (Grt_c), matrix clinopyroxenes (Cpx_1) and matrix plagioclase (Pl_1). In the peak assemblage ($\text{Grt}_c + \text{Cpx}_1 + \text{Pl}_1 + \text{Qz}$), using the geothermometers (Ellis and Green, 1979) and barometers (Eckert et al., 1991) P-T condition ($820 \pm 30^\circ\text{C}$ and 12 ± 0.8 kbar) is determined.

Conventional geothermobarometry (Ellis and Green, 1979; Eckert et al., 1991) of $\text{M}_{1\text{R}1}$ assemblage is done using the garnet rim compositions, and composition of symplectic plagioclase + clinopyroxene. This yields a P-T estimate that converge at $650 \pm 25^\circ\text{C}$ and 7.8 ± 0.5 kbar.

For the conventional thermobarometry of $\text{M}_{1\text{R}2}$ stage Garnet-hornblende thermometry (Graham Powell, 1984) with rim compositions of garnet (Grt_r) and the coexisting amphibole (Amp_2) and Al in amphibole barometry (Anderson and Smith, 1995) is used. These record a temperature in the range of $570 \pm 40^\circ\text{C}$ and constrains the pressure at 6 ± 0.4 kbar.

The measured P-T conditions from early and late retrograde assemblages define a retrograde P-T path of decompression followed by cooling and hydration through the $\text{M}_{1\text{R}1}$ to $\text{M}_{2\text{R}2}$ stages. The estimated peak pressure ($\sim 12 \pm 0.8$ kbar) suggests that the rock suites resided in the lower crust (~ 40 km) during the M_1 stage.

8. Discussion

Petrographic study of the mafic granulites identified four sets of mineral assemblages that represent four different physical conditions experienced by the rocks. Due to the lack preservation of the mineral assemblage and presence of suitable mineral(s), the P-T conditions during which the early assemblage was developed (M_0 stage), could not be determined quantitatively. But quantitative P-T calculation methods could estimate the following physical conditions (M_1 to M_{IR2} stages) for the other three metamorphic assemblages.

Although physical conditions of the early M_0 stage cannot be estimated, the presence of amphibole, plagioclase, quartz and rutile inclusions within the garnet infer that the rock evolved from the amphibole stability field, within the amphibolite facies condition. Thereafter, the rock developed garnets on its way to the peak metamorphic condition along a probable loading path which increases the pressure condition enough to form a peak assemblage of garnet and clinopyroxene. Such assemblages indicate a probable high pressure granulite condition. At the same time, the porphyroblastic grains of garnets and formation of profuse garnets indicate fast growth rate in a dry granulite facies condition. This indicates a synchronous increase of temperature along with pressure.

Gathering all the calculated data and plotting them in a P-T field has been helpful in constructing a probable P-T path. Also from this a tectonic setup can be identified and a broader picture can be drawn describing the different events involved in the evolution of the Chotanagpur Gneissic Complex.

8.1. Plotting the different metamorphic assemblages in the P-T field

The position of the different metamorphic assemblages starting from the peak are shown in the diagram below.

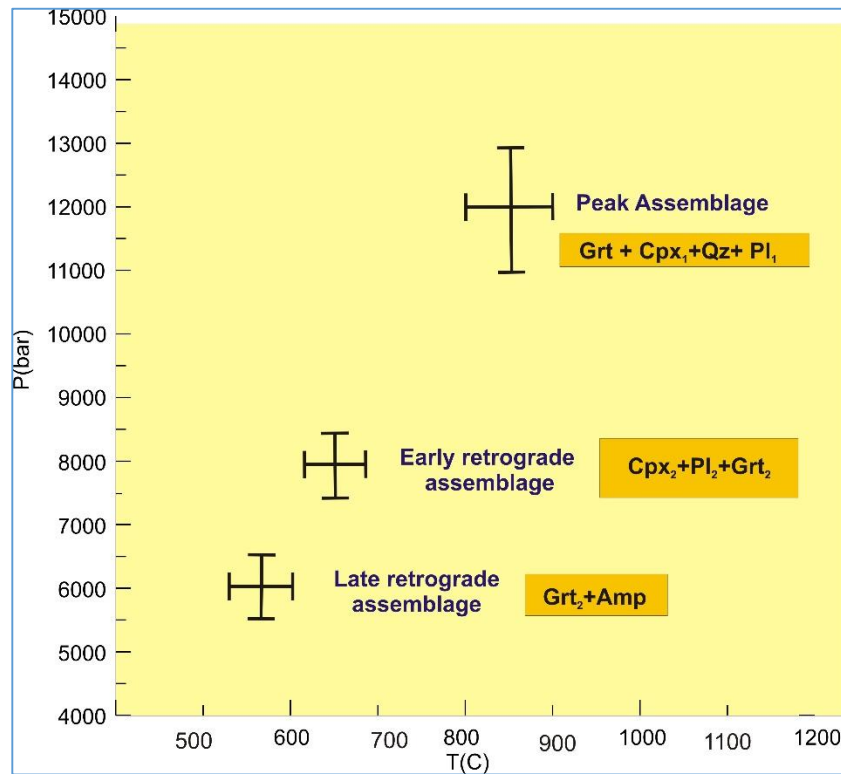


Fig (8) P-T representation of the different metamorphic assemblages.

8.2. Constructing the probable P-T path

Taking the three assemblages as guidelines from the previous diagram, a probable P-T path is constructed.

The inferred prograde path with a steep P-T vector with both pressure and temperature increasing, and the steeply decompressive P-T path originating from the high pressure peak metamorphic stage (M_1) forms a CW P-T path.

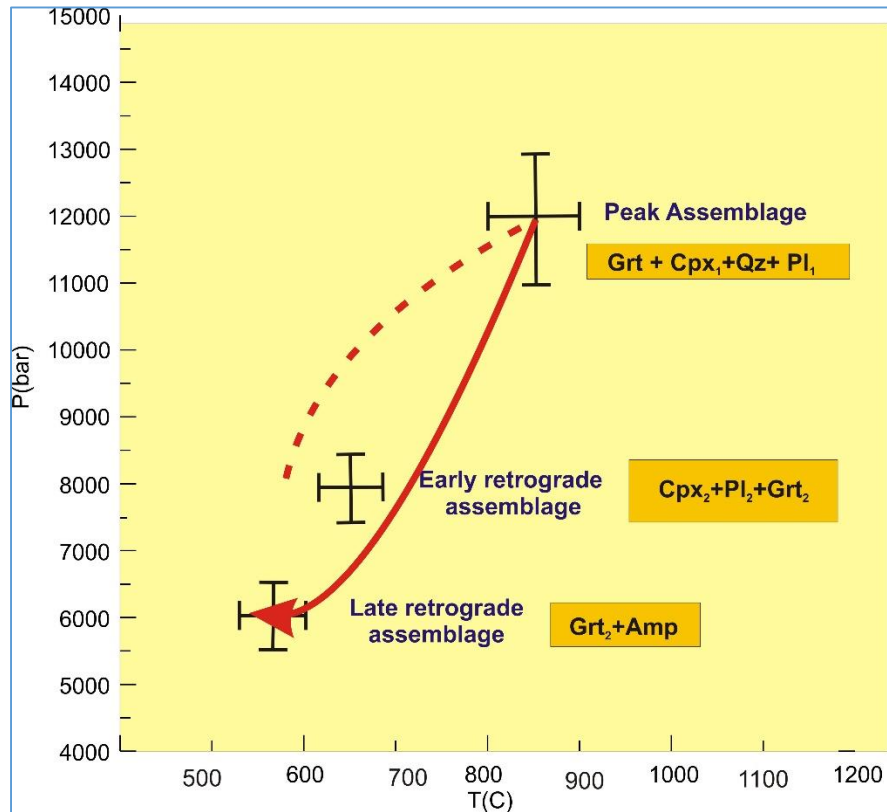


Fig (9) A probable P-T path.

We can see that the retrograde P-T path is a decompressional in nature with significant decrease in pressure at first due to which the early retrograde assemblage (M_{IR1} where dP/dT is 50°C/kbar) is formed followed by a consistent cooling in the late retrograde part (M_{IR2}). This decrease in pressure can be linked with an extension but first the story of the peak assemblage has to be understood. For this the calculated peak metamorphic conditions of the studied rock has to be plotted in the P-T space as a function of different tectonic processes so that we can get an idea about the grade of metamorphism.

8.3. Tectonic implication

The foliation within the mafic granulite enclaves are concordant with the adjacent host felsic country rock. This hints towards simultaneous deformation and metamorphism of these two rock units. Studies have shown that high pressure metamorphism of dominantly felsic crust along a CW P-T path can be best explained by thickening of continental crust during a continent-continent collision (Brown, 2008; Stüwe, 2007).

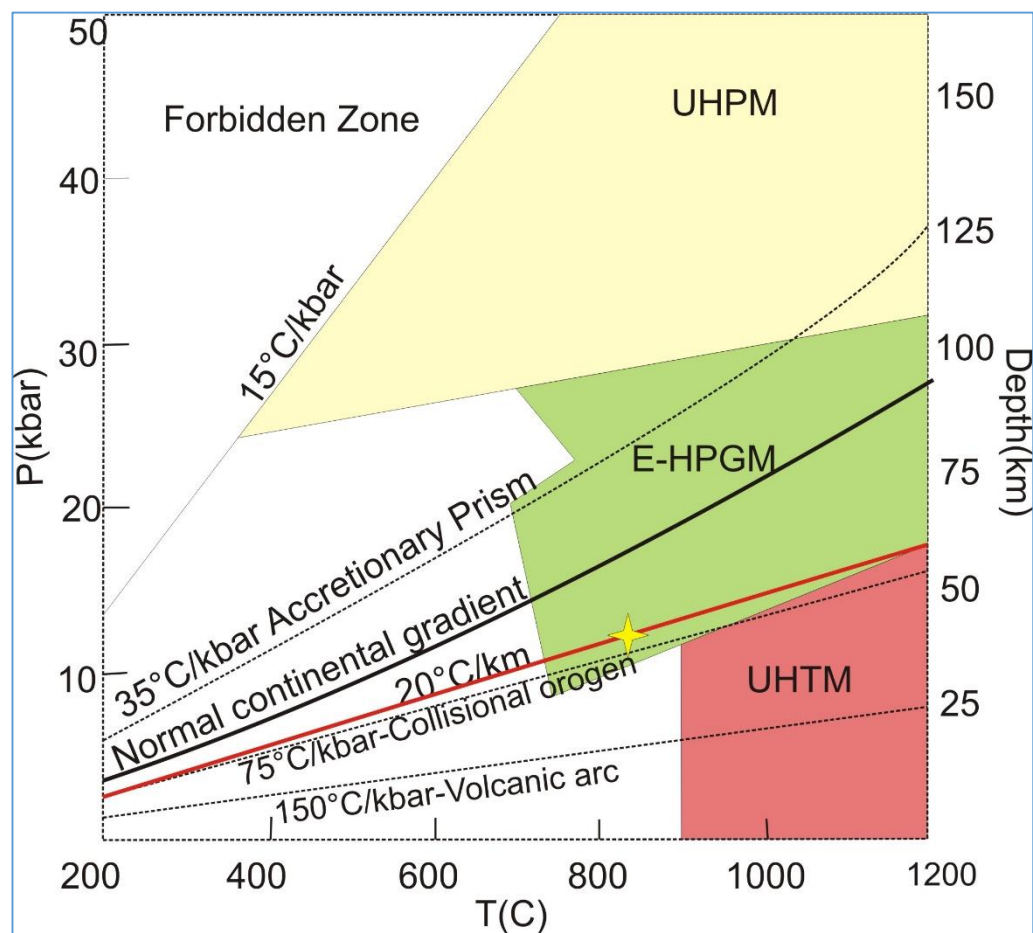


Fig (10) P-T fields as a function of different tectonic process (adapted from Brown, 2008 ; Kelsey and Hand, 2015, Stüwe, 2007)

The calculated peak P-T conditions of the rock ($\sim 12 \pm 1$ kbar, $\sim 820 \pm 30$ °C) plot on the $20^\circ\text{C}/\text{km}$ ($\sim 71^\circ\text{C}/\text{kbar}$) line shown by a star on the above diagram which falls within the field of high pressure granulite metamorphism (HPGM). Coming to the bigger picture, this HPGM can be related to the thickening of the continental crust during a continent-continent collision (CW P-T path) which in turn can be linked with the early Neoproterozoic (950 Ma) collisional event in CGGC (from prior U-Pb zircon dates). Also the probable P-T path established from calculations (Fig. 4) indicates a post peak decompression which seems to represent post-thickening extension bringing the peak metamorphic assemblage from the lower to middle crust (England and Thompson, 1984), as is commonly recorded in convergent orogens (~ 40 km to ~ 26 km, corresponding to a pressure drop from 12 to 7.8 kbar).

The late retrograde assemblage ($dP/dT \sim 40^\circ\text{C}/\text{kbar}$) represents an amphibolite facies metamorphism. The P-T achieved during this stage is sufficient to trigger dehydration and incipient melting in the fertile felsic gneiss. The fluid expelled during from the enclosing gneisses may have induced the hydration of the mafic enclaves in the late stage.

The amphibolite facies M_{1R2} event is extensive in the study area. Whether M_{1R2} was a continuous retrogressive tail of M_1 - M_{1R1} and resulted from a single cycle of tectonism, or a separate amphibolite facies event unrelated to the granulite facies pulse, demands discussion.

From all these a possible evolutionary history of the rocks of the studied area can be reconstructed. This consists of three distinct stages.

Stage 1 (formation of protolith of the mafic granulites)

It has been stated earlier that felsic orthogneisses are the dominant rock types of CGGC containing enclaves of metasedimentary rocks and mafic granulites. The

mafic granulites presumably representing evidence of early mafic magmatism, constitute a very small proportion of the volume. However, certain field features suggest that the protolith of the mafic granulites was emplaced in a continental setting. These include:

(a) Among the other enclaves within the felsic orthogneisses, meta-sedimentary rocks (pelitic and calc-silicate rocks) predominate. Even within a few tens of meters, pods of both meta-sedimentary rocks and mafic granulite are found. This feature suggests that the host rock, in which the protoliths of the mafic enclaves were intruded, was dominantly meta-sedimentary and of a continental shelf affinity (Dey et al., 2017).

(b) Field features show that the meta-sedimentary and the mafic granulite enclaves locally preserve a fabric that developed prior to the emplacement of the younger felsic magma and indicate that both the rock types have an older history of metamorphism and deformation.

In a recent communication, Dey et al. (2017) showed that the oldest fabric of the meta-sedimentary rocks was developed during a metamorphic event at 1640 Ma. On the basis of field relations, it seems likely that the protolith of the mafic granulite was emplaced in a continental setting, pre- to synchronous with this metamorphism. Lack of geochronological data for the mafic rocks is an important drawback in ascertaining the actual age of mafic magmatism.

Stage 2 (intrusion of felsic magma)

In this stage, low pressure melting of the Paleoproterozoic mid-lower crust generated ferroan felsic magmas in an extensional setting under the influence of upwelling

mantle (Mukherjee et al., 2018). These voluminous granitoid plutons intruded the pre-existing continental crust at ~1450 Ma (Mukherjee et al., 2017) and engulfed the meta-sedimentary and mafic rocks which are now found as enclaves of variable dimensions.

Stage 3 (regional deformation and metamorphism)

During this stage, the felsic rocks (the protolith of the felsic orthogneiss) and the enclaves within it developed a strong fabric. The deformation and metamorphism during this stage were so intense that the early fabric and mineralogy of the meta-sedimentary and mafic granulites were obliterated to a large extent. Only in places, where strain was partitioned to the enclosing felsic rocks, the enclaves do preserve vestiges of an older fabric. It should be noted that in the studied mafic rock suite the signature of any older discordant fabric is completely absent; instead, it displays the prominent development of a pervasive younger fabric that is concordant to the migmatitic foliation of the host gneiss. Preservation of a characteristic CW P-T path and geothermal gradient of ~20°–26 °C/km, obtained from mafic granulites and the enclosing felsic orthogneisses (Mukherjee et al., 2017), support the view that both the rock types evolved in a continent-continent collisional setting.

Collisional tectonics of early Neoproterozoic age (~1000-900 Ma) has been reported from worldwide orogenic belts and has been correlated with the formation of the Proterozoic supercontinent Rodinia (Brown, 2007a, 2007b; Li et al., 2008).

The majority of workers have agreed that India was also a part of Rodinia through continental collision between the eastern margin of India (i.e. the Eastern Ghats

mobile belt) and the Rayner province of Antarctica (Dasgupta et al., 2013; Li et al., 2008).

Evidence of typical collisional tectonics of early Neoproterozoic age in India is not restricted to its eastern margin, but also reported from its western (Aravalli Delhi Fold Belt, Bhowmik et al., 2010, 2009; Bose et al., 2017; Saha et al., 2008), central (the Sausar belt, Bhowmik and Roy, 2003; Bhowmik and Spiering, 2004; Roy et al., 2006) and east central (CGGC, Karmakar et al., 2011; Mukherjee et al., 2017) parts. This observation is not only consistent with the traditional view (Li et al., 2008; and others) that India actively participated in the formation of Rodinia, but further more supports that the final amalgamation between the northern and southern Indian blocks took place along the E–W trending composite orogenic belt of the CITZ during Rodinian assembly.

Acknowledgement

It gives me immense pleasure in offering my sincere gratitude to all the persons whose help has made it possible for me to not only complete this work but also made this learning experience truly impounding. I am thankful to the Department of Geological Sciences, Jadavpur University for providing me all sorts of infrastructural facilities which were useful in my thesis work.

First of all I would like to express my heartfelt thanks and deepest regards to my guide and mentor Prof. Sanjoy Sanyal, Department of Geological Sciences, Jadavpur University for helping me all throughout my thesis work. His kind supervision, valuable guidance, cooperation and suggestion at every point have made this thesis work possible. I would also like to thank our research scholar and my senior Somdipta Chatterjee, who was always there to support me with his experience and without whose help this work would not have been complete. I would also like to extend my thanks to Dr. Shreya Karmakar, Dr. Shubham Mukherjee , Dr. Anindita Dey, Sirina Roy Chowdhury, Nivedita Lahiri, Satabdi Das, Enakshi Das, Arimita Chakraborty for their kind help and continuous guidance.

Finally I would like to thank my friend, classmate and lab mate Sayantan Chakraborty who has helped me a lot with the laboratory works and assisted me in every situation.

References

- Bhowmik, S.K., Wilde, S.A., Bhandari, A., Pal, T., Pant, N.C., 2012. Growth of the greater Indian landmass and its assembly in Rodinia: geochronological evidence from the central Indian tectonic zone. *Gondwana Res.* 22, 54–72. <https://doi.org/10.1016/j.gr.2011.09.008>.
- Brown, M., 2007. Metamorphism, plate tectonics, and the supercontinent cycle. *Earth Sci. Front.* 14, 1–18.
- Brown, M., 2007. Metamorphic conditions in orogenic belts: a record of secular change. *Int. Geol. Rev.* 49, 193–234. <https://doi.org/10.2747/0020-6814.49.3.193>.
- Dey, A., Mukherjee, S., Sanyal, S., Ibanez-Mejia, M., Sengupta, P., 2017. Deciphering sedimentary provenance and timing of sedimentation from a suite of metapelites from the Chotanagpur granite gneissic complex, India: implications for proterozoic tectonics in the East-Central part of the Indian shield. In: Mazumder, R (Ed.), *Sediment Provenance; Influences on Compositional Change from Source to Sink*. Elsevier Ltd, pp. 453–486. <https://doi.org/10.1016/B978-0-12-803386-9.00016-2>.
- Droop, G.T.R., 1987. A general equation for estimating Fe³⁺ concentrations in ferromagnesian silicates and oxides from microprobe analyses, using stoichiometric criteria. *Min. Mag.* 51, 431–435. <https://doi.org/10.1180/minmag.1987.051.361.10>.
- Eckert, J.O., Newton, R.C., Kleppa, O.J., 1991. The ΔH of reactions and recalibration of garnet-pyroxene-plagioclase-quartz geobarometers in the CMAS system by solution calorimetry. *Am. Mineral.* 76, 148–160.
- Ellis, D.J., Green, D.H., 1979. An experimental study of the effect of Ca upon garnet-clinopyroxene Fe-Mg exchange equilibria. *Contrib. Mineral. Petrol.* 71, 13–22. <https://doi.org/10.1007/BF00371878>.
- Dey, A., Karmakar, S., Mukherjee, S., Sanyal, S., Dutta, U., & Sengupta, P. (2019). High pressure metamorphism of mafic granulites from the Chotanagpur Granite Gneiss Complex, India: Evidence for collisional tectonics during assembly of Rodinia. *Journal of Geodynamics*. <https://doi.org/10.1016/j.jog.2019.03.005>.

Leake, B.E., Woolley, A.R., Arps, C.E.S., Birch, W.D., Gilbert, M.C., Grice, J.D., Hawthorne, F.C., Kato, A., Kisch, H.J., Krivovichev, V.G., 1997. Report. Nomenclature of amphiboles: report of the subcommittee on amphiboles of the international mineralogical association commission on new minerals and mineral names. *Min. Mag.* 61, 295–321.

Leake, B.E., Woolley, A.R., Birch, W.D., Burke, E.A.J., Ferraris, G., Grice, J.D., Hawthorne, F.C., Kisch, H.J., Krivovichev, V.G., Schumacher, J.C., Stephenson, N.C.N., Whittaker, E.J.W., 2004. Nomenclature of amphiboles: additions and revisions to the International Mineralogical Association's amphibole nomenclature. *Am. Mineral.* 89, 883–887. <https://doi.org/10.1180/0026461046810182>.

Sanyal, S., Sengupta, P., 2012. Metamorphic evolution of the Chotanagpur granite gneiss complex of the East Indian shield: current status. *Geol. Soc. Lond. Spec. Publ.* 365, 117–145. <https://doi.org/10.1144/SP365.7>.

Sengupta, P., Dasgupta, S., Bhui, U.K., Ehlt, J., 1996. Magmatic evolution of mafic granulites from Anakapalle, Eastern Ghats, India: implications for tectonic setting of a Precambrian high-grade terrain. *J. Southeast Asian Earth Sci.* 14, 185–198. [https://doi.org/10.1016/S0743-9547\(96\)00057-8](https://doi.org/10.1016/S0743-9547(96)00057-8).

Spear, F.S., 1991. Temperatures in light of garnet diffusion during cooling. *J. Metamorph. Geol.* 9, 379–388. <https://doi.org/10.1111/j.1525-1314.1991.tb00533.x>.

Spear, F.S., 1993. *Metamorphic Phase Equilibria and Pressure-Temperature-Time Paths*. Monograph 1. Mineralogical Society of America.

Stüwe, K., 1997. Effective bulk composition changes due to cooling: a model predicting complexities in retrograde reaction textures. *Contrib. Mineral. Petrol.* 129, 43–52.

Stüwe, K., 2007. *Geodynamics of the Lithosphere*, 2nd ed. Springer-Verlag, Berlin Heidelberg, <https://doi.org/10.1007/978-3-540-71237-4>.

Zhang J., Zhao G., Sun M., Wilde S.A., Li S., Liu S., 2006. High-pressure mafic granulites in the Trans-North China Orogen: Tectonic significance and age. *Gondwana Research*, 9(3), pp. 349–362.

Zhao, G., Cawood, P.A., Wilde, S.A., Lu, L., 2001. High-pressure granulites (retrograded eclogites) from the Hengshan complex, North China Craton: petrology and tectonic implications. *J. Petrol.* 42, 1141–1170. <https://doi.org/10.1093/petrology/42.6.1141>.

Zhao, G., Wilde, S.A., Cawood, P.A., Lu, L.Z., 2000. Petrology and P – T path of the Fuping mafic granulites: implications for tectonic evolution of the central zone of the North China craton. *J. Metamorph. Geol.* 18, 375–391. <https://doi.org/10.1046/j.1525-1314.2000.00264.x>.

Zhao, G., Cawood, P.A., Wilde, S.A., Lu, L., 2001. High-pressure granulites (retrograded eclogites) from the Hengshan complex, North China Craton: petrology and tectonic implications. *J. Petrol.* 42, 1141–1170. <https://doi.org/10.1093/petrology/42.6.1141>.

Zhao, G., Wilde, S.A., Cawood, P.A., Lu, L., 1999. Thermal evolution of two textural types of mafic granulites in the North China craton: evidence for both mantle plume and collisional tectonics. *Geol. Mag.* 136, 223–240.